

Stationary equilibrium in light of plasma magnetization

Robert W. Johnson

Atlanta, GA 30238, USA

E-mail: rob.johnson@gatech.edu

Abstract. Two extensions of the standard equilibrium equation for magnetized plasma are considered, one β limited and the other with unlimited magnetization. A factor of the pressure gradient arising from the magnetic decomposition survives the limit of vanishing magnetization and is canceled by a contribution from the magnetization force, such that the proposed equations reduce to the standard form in the free current limit. Evaluation of the solutions for an axially symmetric plasma column indicates agreement among the models at weak magnetization and differences at strong magnetization. Current sheet formation is observed in solutions for both the free current and unlimited magnetization models.

PACS numbers: 28.52.-s, 52.30.Ex, 52.55.Fa

Submitted to: *Plasma Phys. Control. Fusion*

1. Introduction

The full effect of plasma magnetization remains poorly understood. From early explorations [1, 2] through modern developments [3, 4], we contend that an important effect has been neglected in the analysis of plasma equilibrium, the magnetization force, despite its experimental applications in fusion [5], magnetic fluids [6, 7, 8], biophysics [9, 10, 11, 12, 13] and materials science [14, 15, 16, 17, 18, 19, 20, 21, 22, 23, 24, 25]. The nonlinear nature of plasma magnetization is often cited as an excuse to neglect it in the usual introductory equilibrium equations [26, 27, 28], which treat the combined bound and free current densities as a single entity; however, we find that the reciprocal relationship between M and H leads to simplifications, rather than complications, in the treatment of stationary equilibrium in a strongly magnetized plasma.

We summarize our notation and assumptions: pure, hydrogenic plasma of species $s \in \{e, i\}$, total particle density $n = n_e + n_i$, total pressure $p = n\mathcal{F} = \sum_s n_s \mathcal{F}_s$, mass density $\rho_m = nm = \sum_s n_s m_s$, current density $\mathbf{J} = \sum_s n_s e_s \mathbf{V}_s$, and vanishing charge density $\rho_e = \sum_s n_s e_s = 0$ and mass velocity $\rho_m \mathbf{V}_m = \sum_s n_s m_s \mathbf{V}_s = 0$, with isotropic pressure $W_s^\perp = 2W_s^\parallel = \mathcal{F}_s$ for $\mathcal{F}_s \equiv k_B T_s$. Our approach to the treatment of magnetization most closely follows that found in References [4, 29, 30], except that we will be fully decomposing the equilibrium equation in terms of \mathbf{H} and \mathbf{M} .

2. Magnetization

The dipole moment per unit volume for each species [4] is taken as $\mathbf{M}_s \equiv n_s \vec{\mu}_s = -n_s (W_s^\perp / B_s) \hat{b}_s$, where the total field felt by species s is $\mathbf{B}_s / \mu_0 = \mathbf{H} + \mathbf{M} - \mathbf{M}_s$ and points along $\hat{b}_s \equiv \mathbf{B}_s / B_s$. The total magnetization of the neutral fluid is given by the dipole density, which for $\tilde{p} \equiv p / \mu_0$ may be written

$$\mathbf{M} \equiv \sum_s \mathbf{M}_s = - \sum_s (n_s W_s^\perp / B_s) \hat{b}_s = - \sum_s (\tilde{p}_s / |\mathbf{H} + \mathbf{M} - \mathbf{M}_s|^2) (\mathbf{H} + \mathbf{M} - \mathbf{M}_s) . \quad (1)$$

How one treats the evaluation of \mathbf{B}_s results in two different models, one β limited and the other with unlimited magnetization. Upon the assumption that the total magnetization is split evenly between the two species e and i , equivalent here to $\mathcal{F}_e = \mathcal{F}_i$ such that $M_s = M/2$, one recovers the equation for the β limit as follows. With $\hat{h} \equiv \mathbf{H} / H$, $\mathbf{B}_s / \mu_0 = (H - M/2) \hat{h}$, and then $\mathbf{M} \equiv -M \hat{h} = -\tilde{p} / (H - M/2) \hat{h}$, which has the physical solution $M = H - \sqrt{H^2 - 2\tilde{p}}$, whence $\beta \equiv 2\tilde{p} / H^2 \leq 1$ else M goes complex enforcing the vanishing of \mathbf{B} , Figure 1. Underlying this model is the reasonable assumption that $M \leq H$ must hold. If we now reconsider our initial definitions formally, for the neutral fluid we have replaced each distinct particle with an ‘‘average’’ particle having mass $m = (m_e + m_i) / 2$ and temperature $(\mathcal{F}_e + \mathcal{F}_i) / 2$. For this ‘‘average’’ species, $M_s = M$ such that $\mathbf{M} = -(\tilde{p} / H) \hat{h}$ and no restriction is placed on the magnitude of the magnetization, which may exceed that of the applied field. One may argue whether such behavior is physically acceptable, yet the procedure is mathematically well defined, thus we will

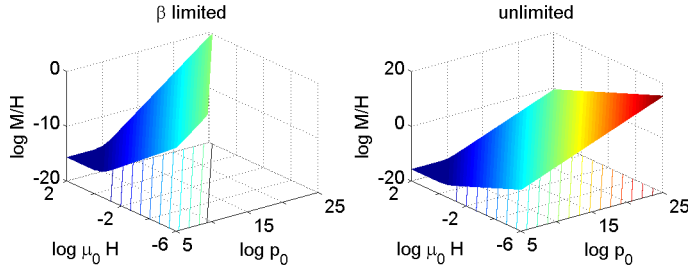


Figure 1. (Color online.) Comparison of the ratio M/H for the β limited and unlimited magnetization models. The central pressure p_0 is in units of keV/m^3 , and the magnetic field $\mu_0 H$ is in units of Tesla. The numerical floor is at $0 \sim O(10^{-16})$ and the β limit is marked by the last black line.

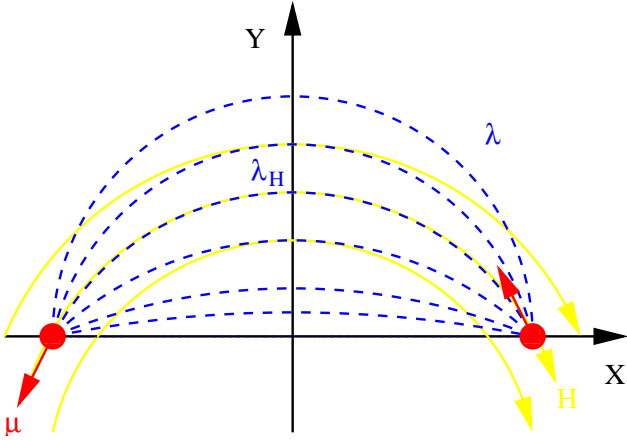


Figure 2. (Color online.) Virtual trajectories λ for the guiding center in a curved magnetic field. The magnitude of $\vec{\mu}$ should be considered fixed and its direction tangential to the guiding center trajectory. The path λ_H along the field line defines a contour of $\vec{\mu} \cdot \mathbf{H}$, hence the force $\mu_0 \nabla(\vec{\mu} \cdot \mathbf{H})$ is everywhere perpendicular to $d\lambda_H$ and the work done $\int_{\lambda_0}^{\lambda_1} d\lambda_H \cdot \mu_0 \nabla(\vec{\mu} \cdot \mathbf{H})$ is zero.

consider both models. Ultimately, the proper treatment of magnetization requires the use of quantum theory [31, 32, 33], in particular as to account for spin.

An infinitesimal dipole $\vec{\mu}$ in an external field \mathbf{H} experiences a force $\mathbf{f} = \mu_0 \nabla(\vec{\mu} \cdot \mathbf{H})$ on the basis of the general theory of magnetized material [29, 31]. This force felt by the guiding center is generalized to the dipole density by $\mathbf{F}_M = \mu_0 \nabla(\mathbf{M} \cdot \mathbf{H})$. We will not yet attempt a kinetic justification for the presence of this term among the moments of the Vlasov equation [3, 4, 27], suggesting that it should be instated at the level of the Boltzmann equation, but rather will explore the consequences on the equilibrium equation of its inclusion, appealing to the mathematically well defined limiting process used in the reductions demonstrated below. The effect of the corresponding force \mathbf{f} on an individual dipole may be understood heuristically as the force of constraint keeping the guiding center on track with its magnetic field line in the thin flux tube picture [34, 35], and the corresponding torque $\mathbf{u} = \mu_0 \vec{\mu} \times \mathbf{H}$ keeps the guiding center aligned, Figure 2. One may argue with our form for the magnetization force \mathbf{F}_M on two grounds, as

for finite gyroradius the expression for the force per particle \mathbf{f} is approximate and as we have chosen to differentiate the dipole density. However, our choice leads to convenient simplifications and may be considered a first step towards a full accounting of magnetization effects on plasma equilibrium.

3. Equilibrium equations

The equilibrium equations we consider are given by

$$\nabla \cdot \mathbf{B}_X = 0, \quad \nabla \times \mathbf{B}_X = \mu_0 \mathbf{J}_X, \quad (2)$$

$$\nabla p = \mathbf{J}_p \times \mathbf{B} + \mu_0 \nabla(\mathbf{M} \cdot \mathbf{H}), \quad (3)$$

where the subscript X appearing in the Maxwell equations identifies the appropriate current source for each component of the magnetic field $\mathbf{B}/\mu_0 \equiv \mathbf{H} + \mathbf{M}$. (Equilibrium in the presence of gravity requires the addition of the gravitational force \mathbf{F}_g to the RHS of the force balance equation above [36].) We require of our proposed equations that they reduce to the standard form $\nabla p = \mathbf{J}_p \times \mathbf{B} = \mu_0(\nabla \times \mathbf{H}) \times \mathbf{H}$ in the limit of vanishing magnetization, which we identify as the free current limit $M \ll H$ such that $J_b \ll J_f$. Note that we will consider taking the limit both before and after evaluation of the differential operators and require agreement in both cases. The total current density is the sum of the external current density and the plasma current density $\mathbf{J} = \mathbf{J}_{ext} + \mathbf{J}_p$, where the plasma current is the sum of the free and bound currents $\mathbf{J}_p \equiv \mathbf{J}_f + \mathbf{J}_b = \nabla \times (\mathbf{H} - \mathbf{H}_{ext}) + \nabla \times \mathbf{M}$, giving us the magnetized equilibrium equation

$$\nabla \tilde{p} = [\nabla \times (\mathbf{H} + \mathbf{M})] \times (\mathbf{H} + \mathbf{M}) + \nabla(\mathbf{M} \cdot \mathbf{H}), \quad (4)$$

where we will retain the magnetization force isolated at the end of our equation and show that it cancels a contribution from the magnetic decomposition which survives the limit of vanishing magnetization $\tilde{p} \ll H^2$, noting that the curl of \mathbf{H}_{ext} is zero within the plasma as well as that the bound current, defined as the curl of the magnetization, remains divergence-free regardless of the geometry and includes the effects of the pressure gradient driven diamagnetic current and the curvature and ∇B drift currents [4]. Note that bound charges and bound currents are physically distinct entities; the former are governed by Gauss's law and associated with the presence of a binding energy between unlike charges while the latter are governed by the Maxwell-Ampere equation [37] and associated with the presence of charges undergoing microscopic circulation. The gyromotion of plasma particles constitutes just such a microscopic circulation and is amenable to treatment as the magnetization of a fluid. The RHS of Equation (3) is our generalization of the macroscopic force densities [38, 39] given by Lorentz and Kelvin, $\mathbf{F}_{LK} = \mu_0 \mathbf{J} \times \mathbf{H} + \mu_0 \mathbf{M} \cdot \nabla \mathbf{H}$, and by Korteweg and Helmholtz, $\mathbf{F}_{KH} = \mathbf{J} \times \mathbf{B} - \mathbf{H} \cdot \mathbf{H} \nabla \mu / 2$. A simplified analysis which neglects the effects of field curvature is presented in the Appendix.

3.1. β limited model

For the β limited model, we consider $M = H(1 - \sqrt{1 - 2\tilde{p}/H^2})$ such that $\mathbf{H} + \mathbf{M} = \mathbf{H}\sqrt{1 - 2\tilde{p}/H^2}$. Manipulation of Equation (4) gives

$$\nabla\tilde{p} = [(\mathbf{H} + \mathbf{M}) \cdot \nabla](\mathbf{H} + \mathbf{M}) - \nabla|\mathbf{H} + \mathbf{M}|^2/2 + \nabla(\mathbf{M} \cdot \mathbf{H}), \quad (5)$$

and upon substitution

$$\nabla\tilde{p} = \left(\mathbf{H}\sqrt{1 - \frac{2\tilde{p}}{H^2}} \cdot \nabla \right) \mathbf{H}\sqrt{1 - \frac{2\tilde{p}}{H^2}} - \frac{1}{2}\nabla \left[H^2 \left(1 - \frac{2\tilde{p}}{H^2} \right) \right] + \nabla(\mathbf{M} \cdot \mathbf{H}), \quad (6)$$

where $\nabla(\mathbf{M} \cdot \mathbf{H}) = -\nabla MH = -\nabla[H^2(1 - \sqrt{1 - 2\tilde{p}/H^2})]$, and we note that the reduction to the standard equation $\nabla\tilde{p} = (\mathbf{H} \cdot \nabla)\mathbf{H} - H\nabla H$ is apparent upon taking the limit. We now consider taking the limit after evaluating the differential operators. The directional derivative term seems not to cause any difficulties, so we will concentrate on the gradient terms. The term $-\nabla|\mathbf{H} + \mathbf{M}|^2/2$ evaluates to

$$-\frac{1}{2}\nabla \left[H^2 \left(1 - \frac{2\tilde{p}}{H^2} \right) \right] = -\nabla (H^2 - 2\tilde{p})/2 = -H\nabla H + \nabla\tilde{p}, \quad (7)$$

and the magnetization force is given by

$$\nabla(\mathbf{M} \cdot \mathbf{H}) = -2H\nabla H + [2(H^2 - \tilde{p})\nabla H - H\nabla\tilde{p}] / \sqrt{H^2 - 2\tilde{p}}, \quad (8)$$

which, upon taking the limit $\tilde{p} \ll H^2$, becomes

$$\nabla(\mathbf{M} \cdot \mathbf{H}) \approx -2H\nabla H + (2H\nabla H - \nabla\tilde{p}) = -\nabla\tilde{p}, \quad (9)$$

and we see that the surviving $\nabla\tilde{p}$ terms cancel such that we recover the standard form. Returning to the term $-\nabla|\mathbf{H} + \mathbf{M}|^2/2$, we find that it evaluates to

$$-\frac{1}{2}\nabla (H - M)^2 = -\frac{1}{2}\nabla (H^2 - 2MH + M^2) = -H\nabla H - M\nabla M + \nabla MH, \quad (10)$$

and that the final term in the equation above is canceled by the magnetization force $\nabla(\mathbf{M} \cdot \mathbf{H}) = -\nabla MH$.

3.2. Unlimited model

Considering now the equilibrium equation for the model with unlimited magnetization $\mathbf{H} + \mathbf{M} = \mathbf{H}(1 - \tilde{p}/H^2)$, upon substitution we find

$$\nabla\tilde{p} = \left[\mathbf{H} \left(1 - \frac{\tilde{p}}{H^2} \right) \cdot \nabla \right] \mathbf{H} \left(1 - \frac{\tilde{p}}{H^2} \right) - \frac{1}{2}\nabla \left(H - \frac{\tilde{p}}{H} \right)^2 + \nabla(\mathbf{M} \cdot \mathbf{H}). \quad (11)$$

Again, the reduction when taking the limit before the evaluation of the operators is apparent, and we focus on the reduction of the gradient terms. The magnetization force becomes simply $\nabla(\mathbf{M} \cdot \mathbf{H}) = -\nabla[(\tilde{p}/H^2)\mathbf{H} \cdot \mathbf{H}] = -\nabla\tilde{p}$, and evaluating the term $-\nabla|\mathbf{H} + \mathbf{M}|^2/2$, we find

$$\nabla\tilde{p} = \left[\mathbf{H} \left(1 - \frac{\tilde{p}}{H^2} \right) \cdot \nabla \right] \mathbf{H} \left(1 - \frac{\tilde{p}}{H^2} \right) - \left(H - \frac{\tilde{p}}{H} \right) \nabla \left(H - \frac{\tilde{p}}{H} \right) + \nabla(\mathbf{M} \cdot \mathbf{H}), \quad (12)$$

wherefrom

$$\nabla\tilde{p} = \left[\mathbf{H} \left(1 - \frac{\tilde{p}}{H^2} \right) \cdot \nabla \right] \mathbf{H} \left(1 - \frac{\tilde{p}}{H^2} \right) \quad (13a)$$

$$-H \left(1 - \frac{\tilde{p}}{H^2} \right) \left(\nabla H + \frac{\tilde{p}}{H^2} \nabla H - \frac{1}{H} \nabla\tilde{p} \right) + \nabla(\mathbf{M} \cdot \mathbf{H}), \quad (13b)$$

and collecting terms

$$\nabla\tilde{p} = \left[\mathbf{H} \left(1 - \frac{\tilde{p}}{H^2} \right) \cdot \nabla \right] \mathbf{H} \left(1 - \frac{\tilde{p}}{H^2} \right) \quad (14a)$$

$$-H \left(1 - \frac{\tilde{p}^2}{H^4} \right) \nabla H + \left(1 - \frac{\tilde{p}}{H^2} \right) \nabla\tilde{p} + \nabla(\mathbf{M} \cdot \mathbf{H}), \quad (14b)$$

which, upon taking the limit $\tilde{p} \ll H^2$, reduces to

$$\nabla\tilde{p} \approx (\mathbf{H} \cdot \nabla) \mathbf{H} - H \nabla H + \nabla\tilde{p} + \nabla(\mathbf{M} \cdot \mathbf{H}), \quad (15)$$

where we have resisted substituting in for the magnetization force $\nabla(\mathbf{M} \cdot \mathbf{H}) = -\nabla\tilde{p}$ to highlight how it cancels the appearance of the pressure gradient in the magnetic decomposition which survives the limit. Returning to Equation (11), we now substitute in our conjectured magnetization force and rewrite the equation using $\tilde{\mathbf{H}} \equiv \mathbf{H}(1 - \tilde{p}/H^2)$, specializing to cylindrical coordinates (r, θ, z) which may be used both for axially symmetric and toroidally symmetric (Z, R, ϕ) configurations,

$$\frac{\partial}{\partial r} \left(2\tilde{p} + \tilde{H}^2/2 \right) = \left(\tilde{H}_r \frac{\partial}{\partial r} + \tilde{H}_\theta \frac{\partial}{r \partial \theta} + \tilde{H}_z \frac{\partial}{\partial z} \right) \tilde{H}_r - \frac{1}{r} \tilde{H}_\theta^2, \quad (16)$$

$$\frac{\partial}{r \partial \theta} \left(2\tilde{p} + \tilde{H}^2/2 \right) = \left(\tilde{H}_r \frac{\partial}{\partial r} + \tilde{H}_\theta \frac{\partial}{r \partial \theta} + \tilde{H}_z \frac{\partial}{\partial z} \right) \tilde{H}_\theta + \frac{1}{r} \tilde{H}_r \tilde{H}_\theta, \quad (17)$$

$$\frac{\partial}{\partial z} \left(2\tilde{p} + \tilde{H}^2/2 \right) = \left(\tilde{H}_r \frac{\partial}{\partial r} + \tilde{H}_\theta \frac{\partial}{r \partial \theta} + \tilde{H}_z \frac{\partial}{\partial z} \right) \tilde{H}_z. \quad (18)$$

Retaining only the gradient terms is valid provided $(\mathbf{B} \cdot \nabla)\mathbf{B} \approx 0$.

4. Evaluation

Restricting consideration to an axially symmetric plasma column with $\partial/\partial\theta \equiv \partial/\partial z \equiv 0$ embedded in a constant external magnetic field $\mathbf{H}_{ext} = H_{ext}^0 \hat{z}$, the free current within the plasma is here supposed to be purely axial $\mathbf{J}_f = J_z(r) \hat{z}$, giving rise to an azimuthal magnetic field $\mathbf{H}_f = H_\theta(r) \hat{\theta}$. The applied field $\mathbf{H} = \mathbf{H}_{ext} + \mathbf{H}_f$ satisfies $\nabla \cdot \mathbf{B} = 0$, leaving us to evaluate Equations (6) and (16), whereupon manipulation gives us the β limited equation

$$3H_\theta \frac{\partial H_\theta}{\partial r} - \left[2 \left(1 - \frac{\tilde{p}}{H^2} \right) H_\theta \frac{\partial H_\theta}{\partial r} - \frac{\partial \tilde{p}}{\partial r} \right] \left(1 - \frac{2\tilde{p}}{H^2} \right)^{-1/2} = -\frac{1}{r} \left(1 - \frac{2\tilde{p}}{H^2} \right) H_\theta^2, \quad (19)$$

and the unlimited magnetization equation

$$\left(1 + \frac{\tilde{p}}{H^2} \right) \frac{\partial \tilde{p}}{\partial r} + \left(1 - \frac{\tilde{p}}{H^2} \right) \left(1 + \frac{\tilde{p}}{H^2} \right) H_\theta \frac{\partial H_\theta}{\partial r} = -\frac{1}{r} \left(1 - \frac{\tilde{p}}{H^2} \right)^2 H_\theta^2, \quad (20)$$

which are invariant under the transformation $H_\theta \rightarrow -H_\theta$, corresponding to the two possible orientations for the axial current. The unmagnetized free current model equilibrium equation, which is also unlimited, reduces to

$$\frac{\partial \tilde{p}}{\partial r} + H_\theta \frac{\partial H_\theta}{\partial r} = -\frac{1}{r} H_\theta^2, \quad (21)$$

and our problem is defined as: given $p(r)$, find $H_\theta(r)$. Parametrizing the pressure of a plasma column of meter radius by $p = p_0(1 - r^a)$ with constant $a > 0$, we compare the magnetized and unmagnetized solutions for the parabolic $a = 2$ profile with a central pressure p_0 of 10^{20} to 10^{22} keV/m³ in an external field which decreases from 1T down to .1T, Figure 3, where we find the expected agreement among the three models in the limit of weak magnetization with low central pressure and strong external field, and we note the formation of current sheets for the unlimited models as evidenced by sharp increases in the azimuthal field for both solutions. The unlimited magnetization solutions support the formation of current sheets at a stronger external field than the unmagnetized solutions, and the β limited solutions do not exist beyond the β limit. For most of the parameters considered in the figure, we see that the unlimited magnetized and unmagnetized solutions have the same azimuthal field at the boundary, hence equivalent total free plasma currents $I_f = 2\pi H_\theta(r = 1)$ which could not be distinguished by an external measurement, yet a region in parameter space beyond the β limit does appear in which the two solutions may be experimentally distinguished. We explore that region by computing I_f as a function of H_z in Figure 4, finding an opportunity to distinguish the models at a p_0 of 10^{21} keV/m³ for an external field $\mu_0 H_z$ around 10mT, and we also compare the relations for I_f as a function of p_0 in Figure 5, where the models have different predictions for an external field $\mu_0 H_z \lesssim .1$ T, thus our conjectured extensions to the usual equilibrium equation may be put directly to test for plasmas beyond the β limit.

Satisfied that the unlimited magnetization model reproduces the physics of the standard equilibrium equation in the appropriate limit, we now conduct an evaluation of the effects of the shape of the pressure profile on the magnetized equilibrium. For central pressures p_0 of 10^{18} to 10^{22} keV/m³, we find the solution H_θ , its associated flux function $d\Psi \equiv H_\theta dr$, and the axial free current density $J_z = [\nabla \times \mathbf{H}_f]_z = H_\theta/r + \partial H_\theta/\partial r$, for $.1 \leq a \leq 4$ with $\mu_0 H_z = .2$ T. In Figures 6 through 10 we display the normalized profiles, noting the smooth transition to the current sheet configuration as the central pressure increases. We also observe that the relation between p and Ψ need not be a simple one, especially for a strongly magnetized plasma, as the steep gradient in Ψ at the location of the current sheet separating a region of weak azimuthal field from that of a strong one requires better than a low-order polynomial approximation for $dp/d\Psi$ —the implications for the determination of flux surface geometry in toroidal configurations for plasmas beyond the β limit from solution of the usual Grad-Shafranov equation [40, 41] is worrisome, and more investigation in this regard is warranted. Finally, we evaluate the relation between I_f and a by plotting $\tilde{I}_f \equiv I_f(\sqrt{a})/I_f(a_{max})$ for p_0 over 10 orders of magnitude 10^{14} to 10^{24} keV/m³ as $\mu_0 H_z$ decreases from 1T down to .05T, Figure 11.

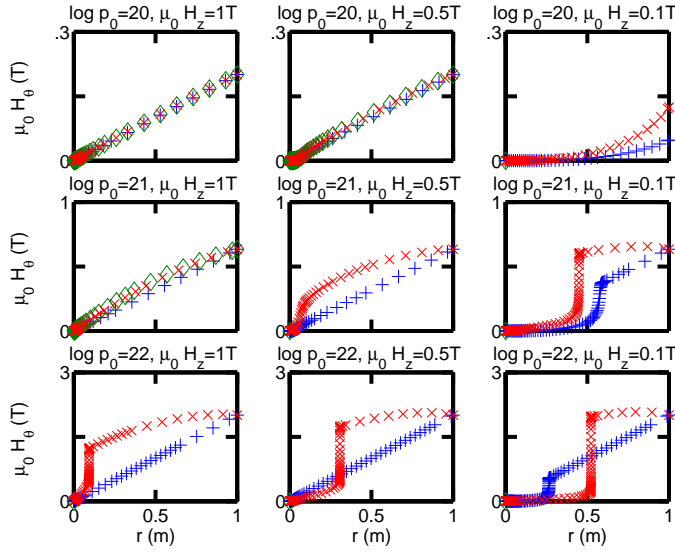


Figure 3. (Color online.) Comparison of the solutions H_θ for the parabolic pressure profile $a = 2$ at several levels of magnetization. The central pressure p_0 is in units of keV/m^3 . The free current model is given by $+$, the unlimited magnetization model by \times , and the β limited model by \diamond when $p_0 < \mu_0 H_z^2/2$, and the three models agree in the limit of vanishing magnetization. The free current and unlimited models have equivalent azimuthal fields at the boundary for most of the parameters displayed, and the formation of the current sheet is more pronounced for the magnetized equilibrium and can occur at greater external field strength.

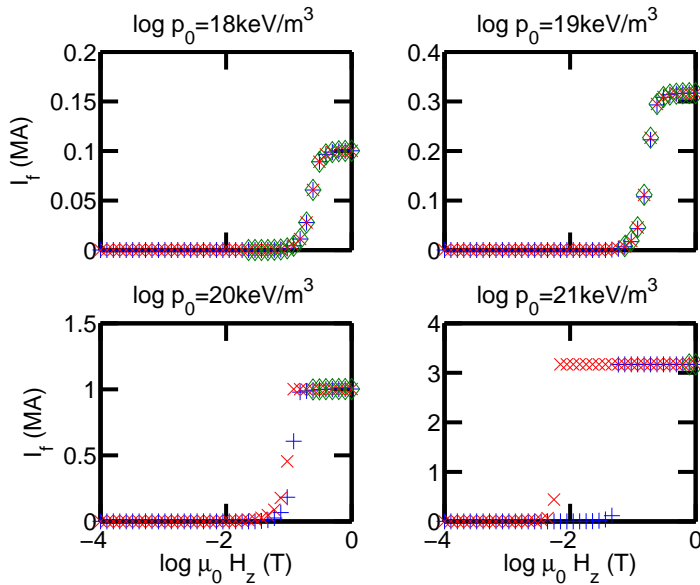


Figure 4. (Color online.) Comparison of the relation between total free current I_f and external field H_z for the parabolic pressure profile $a = 2$. The free current model is given by $+$, the unlimited magnetization model by \times , and the β limited model by \diamond when $p_0 < \mu_0 H_z^2/2$. All three models give equivalent I_f below the β limit, and for $p_0 = 10^{21} \text{keV}/\text{m}^3$ a window of opportunity opens for an external field around 10mT to distinguish the free current and unlimited magnetization models.

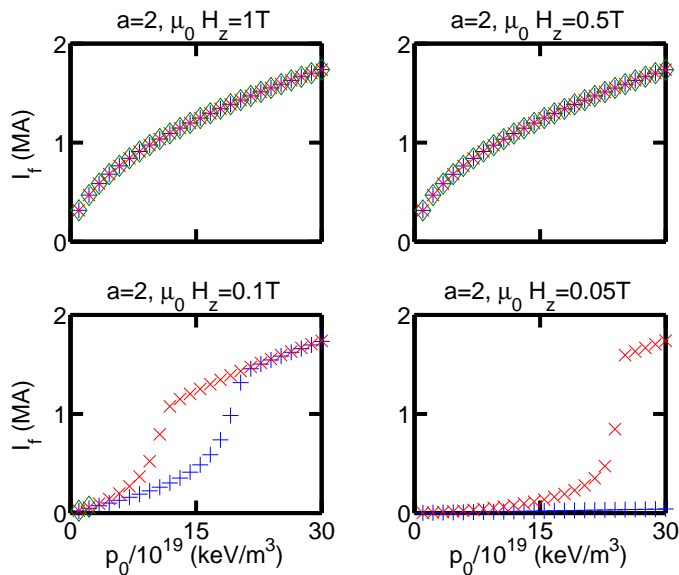


Figure 5. (Color online.) Comparison of the relation between total free current I_f and central pressure p_0 for the parabolic pressure profile $a = 2$. The free current model is given by +, the unlimited magnetization model by \times , and the β limited model by \diamond when $p_0 < \mu_0 H_z^2/2$. Note that for $\mu_0 H_z \lesssim .1\text{T}$ the models become distinguishable.

Here we find that $\tilde{I}_f^2 \propto a$ for a strong external field and that a different relation holds for lower central pressures in a weaker field—for the weakest field shown, the transition from the curved line to the straight line occurs for p_0 between 10^{18} and 10^{19}keV/m^3 . The same relation is found to hold for the unmagnetized equilibrium in the free current limit for the range of parameters considered.

5. Conclusion

In conclusion, we have determined that our conjectured form for the magnetization force provides just the right cancellation required to take the magnetically decomposed $\mathbf{H} + \mathbf{M}$ equilibrium equation over to the usual equation in the free current limit $M \ll H$ for either choice of magnetization model. We wonder if previous investigators, when confronted with that extra term ∇p upon taking the limit of the magnetically decomposed equation without inclusion of the magnetization force, were stymied as to how to proceed. By providing the necessary balance, the magnetization force allows for the extension of the standard theory into the strongly magnetized regime. When compared to solutions of the usual equation, we find exact agreement in the limit of vanishing magnetization and recover interesting variations for the location of the current sheet as magnetization effects become more pronounced. We also have found that the relation between the pressure profile and the flux function need not be a simple one for a plasma beyond the β limit. A scaling relation is found between the total free axial current and the parameter of the pressure profile which holds over 10 orders of magnitude in central pressure for a strong external field and which needs

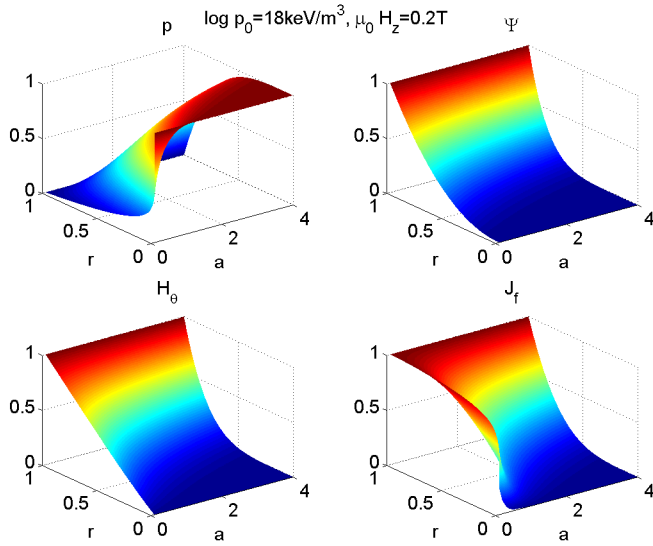


Figure 6. (Color online.) Comparison of the normalized profiles for pressure p , flux function Ψ , azimuthal field H_θ , and axial current density J_z for the unlimited magnetization model with $\mu_0 H_z = .2\text{T}$ and $p_0 = 10^{18}\text{keV/m}^3$. Note that the maximum current density occurs at the outer boundary.

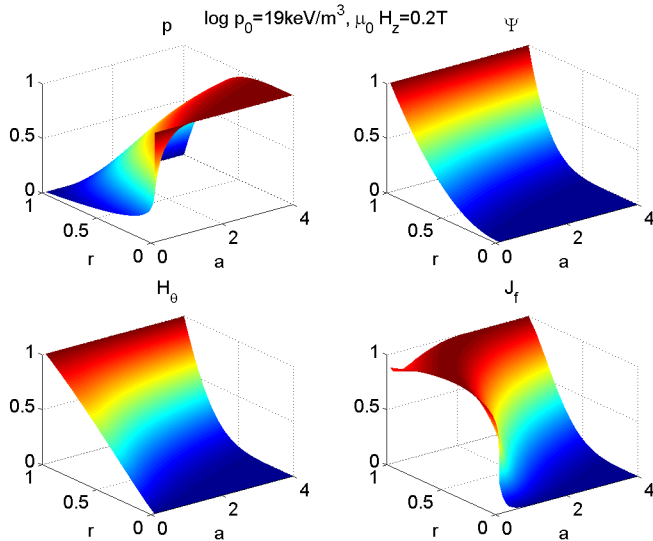


Figure 7. (Color online.) Comparison of the normalized profiles for pressure p , flux function Ψ , azimuthal field H_θ , and axial current density J_z for the unlimited magnetization model with $\mu_0 H_z = .2\text{T}$ and $p_0 = 10^{19}\text{keV/m}^3$. Note that the maximum current density has moved in from the outer boundary for peaked pressure profiles $a < 2$.

adjustment for lower pressures in a weaker field. A region in the parameter space is found where the magnetized and unmagnetized equilibrium equations may be put up against experimental measurements.

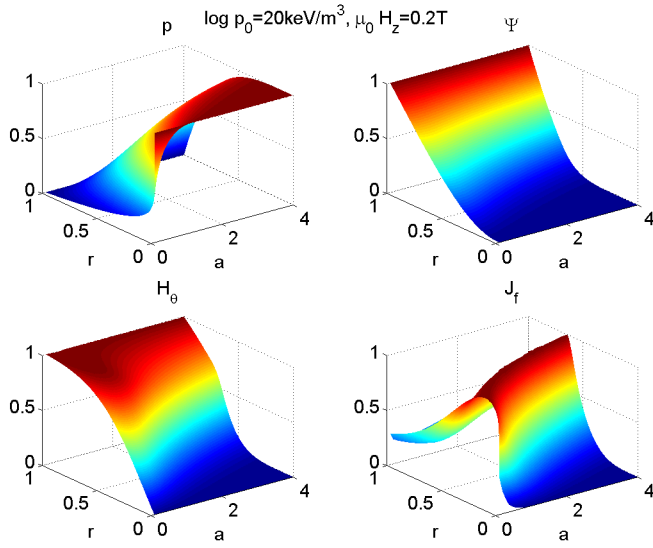


Figure 8. (Color online.) Comparison of the normalized profiles for pressure p , flux function Ψ , azimuthal field H_θ , and axial current density J_z for the unlimited magnetization model with $\mu_0 H_z = .2\text{T}$ and $p_0 = 10^{20}\text{keV/m}^3$. Note the formation of a current sheet has begun for the entire range of a displayed.

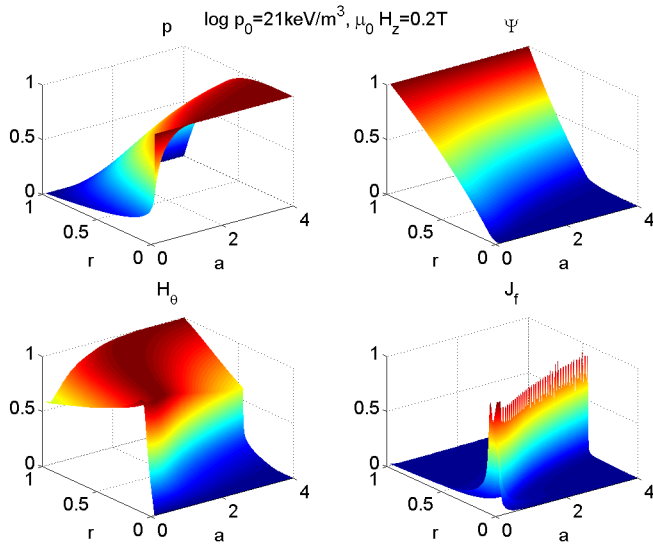


Figure 9. (Color online.) Comparison of the normalized profiles for pressure p , flux function Ψ , azimuthal field H_θ , and axial current density J_z for the unlimited magnetization model with $\mu_0 H_z = .2\text{T}$ and $p_0 = 10^{21}\text{keV/m}^3$. Note the formation of a distributed current sheet for the entire range of a displayed. The jaggedness in the plot is a rendering artifact.

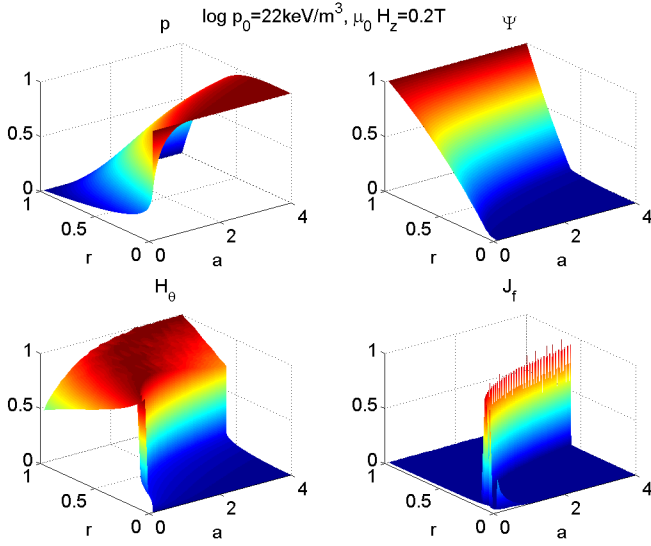


Figure 10. (Color online.) Comparison of the normalized profiles for pressure p , flux function Ψ , azimuthal field H_θ , and axial current density J_z for the unlimited magnetization model with $\mu_0 H_z = .2\text{T}$ and $p_0 = 10^{22}\text{keV/m}^3$. Note the formation of a sharp current sheet for the entire range of a displayed. The jaggedness in the plot is a rendering artifact.

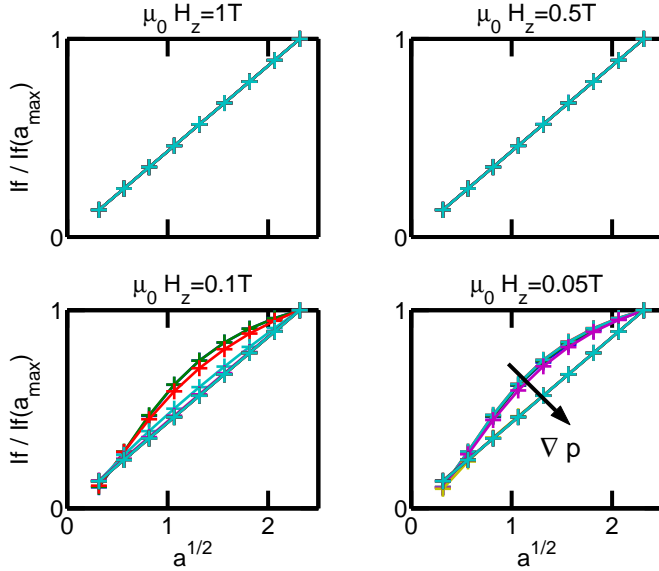


Figure 11. (Color online.) Comparison of the unlimited model's scaling relation between the normalized total free axial current $\tilde{I}_f \equiv I_f(\sqrt{a})/I_f(a_{\max})$ and pressure profile parameter a over 10 orders of magnitude 10^{14} to 10^{24}keV/m^3 in central pressure p_0 for strong and weak external field strength. For the weakest field displayed, the transition from the curved line to the straight line occurs for p_0 between 10^{18} and 10^{19}keV/m^3 . The same relation is found to hold for the free current model as well, with just a slightly different rate through the transition region. Animations of the profiles used in this evaluation are available online.

Appendix A. Equilibrium neglecting field curvature

With specialization to consideration of an axisymmetric plasma column in (r, θ, z) coordinates with azimuthal and axial symmetry $\partial/\partial\theta \equiv \partial/\partial z \equiv 0$ embedded in an external magnetic field which is axial and constant $\mathbf{B}_{ext} = B_{ext}^0 \hat{z}$. The free current within the plasma is supposed to be purely axial $\mathbf{J}_f = J_f(r) \hat{z}$, giving rise to an azimuthal magnetic field $\mathbf{B}_f = B_f(r) \hat{\theta}$. The applied field $\mu_0 \mathbf{H} = (0, B_f, B_{ext})$ satisfies $\nabla \cdot \mathbf{B} = 0$ as well as $(\mathbf{B} \cdot \nabla) \mathbf{B} \approx 0$, leaving us with

$$\nabla \left[2p + \frac{\mu_0}{2} \left(H_M - \frac{\tilde{p}}{H_M} \right)^2 \right] \approx 0, \quad (\text{A.1})$$

for the unlimited magnetization model $\mathbf{F}_M = -\nabla p$, wherefrom

$$2\tilde{p} + \frac{1}{2} \left(H_M - \frac{\tilde{p}}{H_M} \right)^2 = C_M, \quad (\text{A.2})$$

with constant C_M evaluated from the boundary condition at the center $r = 0$, an algebraic equation. The physical solution is given by $H_M = \sqrt{(C_M/2 - \tilde{p})} + \sqrt{C_M/2}$, from which we determine the azimuthal field $B_f^M = \sqrt{\mu_0^2 H_M^2 - B_{ext}^2}$ and axial current density $J_f^M = [\nabla \times \mathbf{H}_M]_z$. This solution may be compared to that without magnetization,

$$\tilde{p} + H_0^2/2 = C_0. \quad (\text{A.3})$$

For a plasma with radius 1 meter in an external field B_{ext} of 1 Tesla and a central density n_0 of $10^{19}/\text{m}^3$, we consider the pressure profiles $p = n_0 \mathcal{F}_0 (1 - r^a)$ parametrized by $a > 0$ and core temperature \mathcal{F}_0 . We compute the solutions H_M and H_0 , and in Figure A1 we display the differences $\Delta J_f \equiv J_f^M - J_f^0$ and $\mu_0 \Delta H_\theta \equiv \mu_0 (H_\theta^M - H_\theta^0)$. For the parabolic pressure profile $a = 2$ at a core temperature of $\mathcal{F}_0 = 10\text{keV}$, the magnetized equilibrium requires up to 1 millitesla more azimuthal field than the unmagnetized equilibrium, corresponding to an increase in the axial current density of a few kA/m². We note that increasing temperature also increases the magnetization, requiring more additional axial current for equilibrium. We also note that a peaked pressure profile $a \lesssim 1$ requires much greater current on the axis than profiles with a more distributed pressure core $a > 1$.

One might question whether the factor of 2 on the pressure gradient appearing in Equations (A.1) and (A.2) coming from the magnetization force is physical. To evaluate its effect, we compare the solution of the magnetized Equation (A.2) with the magnetization force, including consideration of an error in its sign, to the magnetized solution without the magnetization force and with the unmagnetized solution to Equation (A.3) for several pressure profiles in a decreasing external field and by evaluating the total enclosed free plasma current $I_f = 2\pi H_\theta(r = 1)$ as a function of central temperature for the parabolic pressure profile with central density $10^{19}/\text{m}^3$. Neglecting the magnetization force changes the coefficient of the pressure term in Equation (A.2) to unity. Returning to Equation (A.1), we explicitly evaluate the derivative to obtain

$$\frac{\partial}{\partial r} \left[2\tilde{p} + \frac{1}{2} \left(H - \frac{\tilde{p}}{H} \right)^2 \right] = 2 \frac{\partial \tilde{p}}{\partial r} + H \left(1 - \frac{\tilde{p}}{H^2} \right) \left[\left(1 + \frac{\tilde{p}}{H^2} \right) \frac{\partial H}{\partial r} - \frac{1}{H} \frac{\partial \tilde{p}}{\partial r} \right], \quad (\text{A.4})$$

$$\approx \frac{\partial \tilde{p}}{\partial r} + H_\theta \frac{\partial}{\partial r} H_\theta . \quad (\text{A.5})$$

Note that if one chooses to neglect the factor of \tilde{p}/H going into the LHS of the equation above, then one has to remove the factor of 2 by definition—the evaluation above demonstrates that the RHS of the magnetized equation reduces to the standard form in the appropriate limit. One may parametrize our options for the magnetized Equation (A.2) by replacing the factor of 2 on the pressure \tilde{p} with the constant C_p defined by

$$C_p \equiv \begin{cases} 2 & , \quad \mathbf{F}_M = -\nabla p \\ 1 & , \quad \mathbf{F}_M = 0 \\ 0 & , \quad \mathbf{F}_M = +\nabla p \end{cases} , \quad (\text{A.6})$$

where $C_p = 0$ accounts for flipping the sign of \mathbf{F}_M . Our comparison of $\mu_0 H_\theta(r)$ for the various options is presented in Figure A2, where we find that only $C_p = 2$ is compatible with the solution of the unmagnetized equation. In Figure A3 we display the comparison of the total plasma current I_f for an external field which decreases from 1T down to .05T, neglecting the case $C_p = 0$. We find that the magnetized solution with the magnetization force $\mathbf{F}_M = -\nabla p$ agrees with the unmagnetized solution for a strong external field, while the magnetized solution without the magnetization force does not, which is not at all surprising in light of the preceding arguments. We note that for $B_z = .1\text{T}$ the unmagnetized solution agrees with the magnetization force solution at high central temperature and follows more closely the solution without the magnetization force at lower central temperature. For the lowest external field displayed, .05T, we note the clear distinction between the solutions as the central temperature approaches 30keV, indicating a possible means to determine experimentally the correct form of the equilibrium equation for a strongly magnetized plasma.

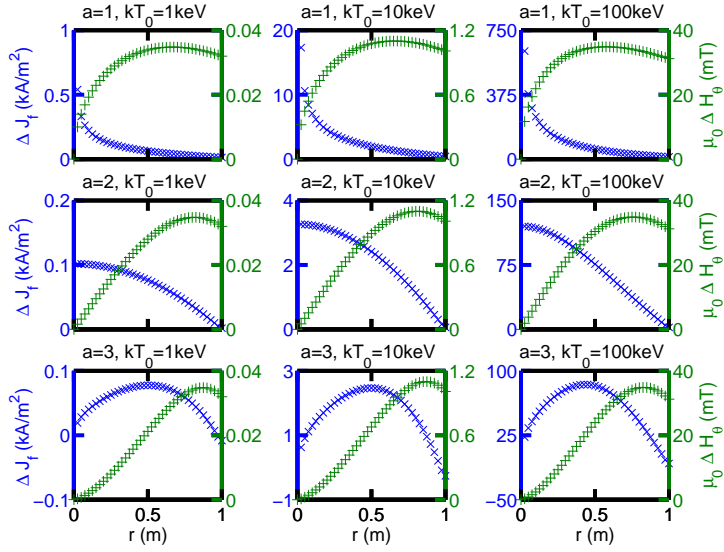


Figure A1. (Color online.) The effect of plasma magnetization displayed as the increase in axial current density $\Delta J_f \equiv J_f^M - J_f^0$, \times , and azimuthal field $\mu_0 \Delta H_\theta \equiv \mu_0 (H_\theta^M - H_\theta^0)$, $+$, over the unmagnetized equilibrium for the algebraic formulation. The current axes are on the left in units of 10^3A/m^2 , and the magnetic field axes are on the right in units of 10^{-3}T . The pressure profile $p(r) = p_0(1 - r^a)$ is parametrized by a and central temperature kT_0 for central density $n_0 = 10^{19}/\text{m}^3$ and external field $B_{ext} = 1 \text{T}$.

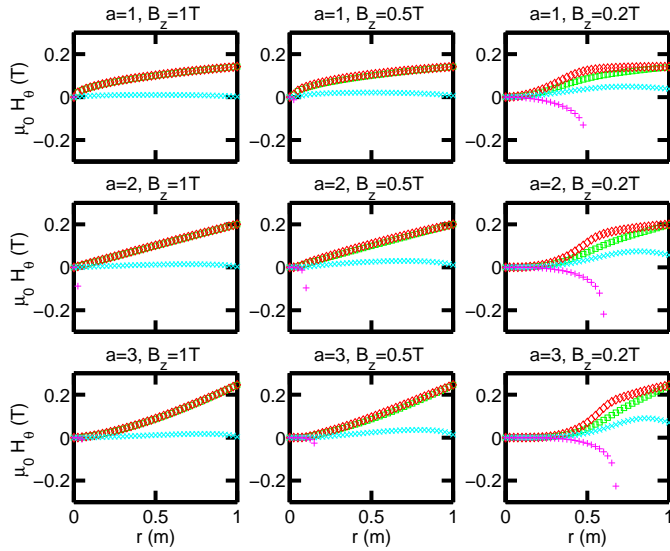


Figure A2. (Color online.) Comparison of the various options for the magnetization force in the magnetized equation compared to the standard solution in the free-current limit for a central pressure of $10 \text{keV} \times 10^{19}/\text{m}^3$ in a decreasing external field. The standard unmagnetized solution is given by \square and for C_p defined in the text, $C_p = 2$ is given by \diamond , $C_p = 1$ is given by \times , and $C_p = 0$ is given by $+$. We note that $C_p = 2$ is the only option compatible with the unmagnetized solution.

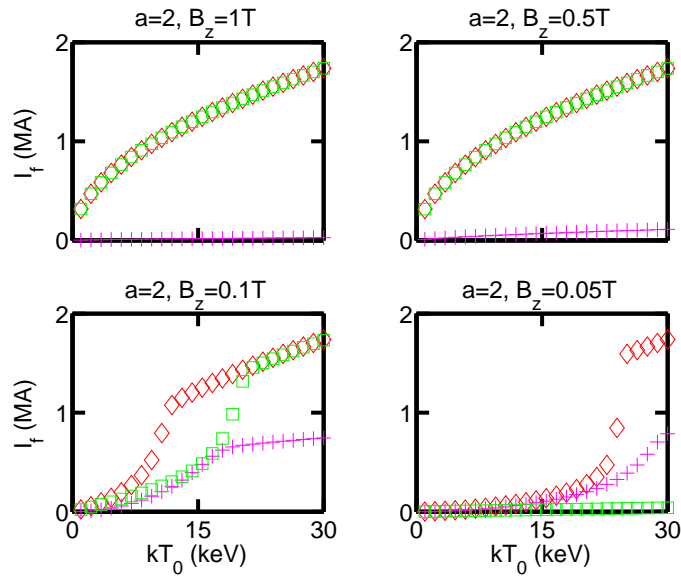


Figure A3. (Color online.) The effect of the magnetization force $\mu_0 \nabla(\mathbf{M} \cdot \mathbf{H})$ on the total enclosed plasma free current I_f for the parabolic pressure profile with a central density of $10^{19}/\text{m}^3$ as a function of central temperature \mathcal{T}_0 displayed for decreasing external magnetic field B_z . The magnetized solution with the magnetization force $C_p = 2$ is given by \diamond , the magnetized solution without the magnetization force $C_p = 1$ by $+$, and the unmagnetized solution by \square . Note that the magnetized solution with the magnetization force agrees with the unmagnetized solution for a strong external field while the magnetized solution without the magnetization force does not.

- [1] J. R. Roth. Plasma stability and the Bohr - van Leeuwen theorem. Technical Report NASA TN D-3880, National Aeronautics and Space Administration, April 1967.
- [2] Laurence S. Hall. Plasma magnetization and the determination of hydromagnetic equilibrium. *Physics of Fluids*, 15(4):710–712, 1972.
- [3] R. D. Hazeltine and J. D. Meiss. *Plasma Confinement*. Courier Dover Publications, 2003.
- [4] R. D. Hazeltine and F. L. Waelbroeck. *The Framework of Plasma Physics*. Westview Press, 2004.
- [5] M. A. Hayes, M. R. Brown, T. E. Sheridan, R. L. Abraham, and M. A. Kasevich. Current drive from rf-induced modulation of plasma magnetization. *AIP Conference Proceedings*, 129(1):213–217, 1985.
- [6] C. Rinaldi and M. Zahn. Effects of spin viscosity on ferrofluid flow profiles in alternating and rotating magnetic fields. *Physics of Fluids*, 14:2847–2870, August 2002.
- [7] M. Zahn and L. L. Pioch. Ferrofluid flows in AC and traveling wave magnetic fields with effective positive, zero or negative dynamic viscosity. *Journal of Magnetism and Magnetic Materials*, 201:144–148, 1999.
- [8] Yusry O. El-Dib and Galal M. Moatimid. The instability of a viscoelastic conducting cylindrical interface supporting free-surface currents. *Zeitschrift fr Naturforschung. A*, 57(3-4):159–176, 2002.
- [9] E. E. Tzirtzilakis. A mathematical model for blood flow in magnetic field. *Physics of Fluids*, 17(7):077103, 2005.
- [10] N. Ramachandran and F. W. Leslie. Using magnetic fields to control convection during protein crystallization—analysis and validation studies. *Journal of Crystal Growth*, 274(1-2):297–306, 2005.
- [11] J. Qi, N. I. Wakayama, and M. Ataka. Magnetic suppression of convection in protein crystal growth processes. *Journal of Crystal Growth*, 232:132–137(6), November 2001.
- [12] Mitsuo Ataka and Nobuko I. Wakayama. Effects of a magnetic field and magnetization force on protein crystal growth. Why does a magnet improve the quality of some crystals? *Acta Crystallographica Section D*, 58(10 Part 1):1708–1710, Oct 2002.
- [13] L. B. Wang and N. I. Wakayama. Effects of strong magnetic fields on natural convection in the vicinity of a growing cubic protein crystal. *ISIJ International*, 43(6):877–883, 2003.
- [14] Syou Maki and Mitsuo Ataka. Effects of non-axisymmetric magnetization force on natural convection of water at various off-centered positions in superconducting magnet: Numerical computation studies. *Jpn. J. Appl. Phys.*, 44:1132–1138, 2005.
- [15] Syou Maki, Mitsuo Ataka, Toshio Tagawa, Hiroyuki Ozoe, and Wasuke Mori. Natural convection of a paramagnetic liquid controlled by magnetization force. *AIChE Journal*, 51(4):1096–1103, 2005.
- [16] Syou Maki and Mitsuo Ataka. Magnetization force sensor. *Review of Scientific Instruments*, 76(6):066106, 2005.
- [17] Y. Ma, L. Xiao, and L. Yan. Application of high magnetic field in advanced materials processing. *Chinese Science Bulletin*, 51(24):2944–2950, 2006.
- [18] Shigeo Asai. Application of high magnetic fields in inorganic materials processing. *Modelling and Simulation in Materials Science and Engineering*, 12(2):R1–R12, 2004.
- [19] Tsutomu Takagi, Kazuhiko Iwai, and Shigeo Asai. Solidified structure of Al alloys by a local imposition of an electromagnetic oscillation force. *ISIJ Int.*, 43(6):842–848, 2003.
- [20] Toshiyuki Kozuka, Toyohiro Sakai, Reiko Miyamura, and Masayasu Kawahara. Effect of magnetic convection on metal substitution reaction under intense magnetic field. *ISIJ International*, 43(6):884–889, 2003.
- [21] Fangwei Jin, Zhongming Ren, Weili Ren, Kang Deng, Yunbo Zhong, and Jianbo Yu. Effects of a high-gradient magnetic field on the migratory behavior of primary crystal silicon in hypereutectic Al–Si alloy. *Science and Technology of Advanced Materials*, 9(2):024202 (6pp), 2008.
- [22] Fabrizio Colli, Massimo Fabbri, Francesco Negrini, Shigeo Asai, and Kensuke Sassa. Removal of SiC inclusions in molten aluminium using a 12T static magnetic field. *COMPEL*:

- The International Journal for Computation and Mathematics in Electrical and Electronic Engineering*, 22(1):58 – 67, 2003.
- [23] Takuya Ono, Kensuke Sassa, Kazuhiko Iwai, Hideyuki Ohtsuka, and Shigeo Asai. Quantification of isothermal phase transformation in solid metals based on measurement of magnetic susceptibility. *ISIJ International*, 47(4):608–611, 2007.
- [24] B. Cantor and K. O’Reilly. *Solidification and Casting*. CRC Press, 2002.
- [25] Frerich Johannes Keil. *Modeling of Process Intensification*. Wiley-VCH, 2007.
- [26] F. F. Chen. *Introduction to Plasma Physics and Controlled Fusion*. Springer, 1984.
- [27] R. Dendy. *Plasma Physics: an Introductory Course*. Cambridge University Press, Cambridge, England, 1993.
- [28] Weston M. Stacey. *Fusion Plasma Physics*. Wiley-VCH, 2005.
- [29] D. Griffiths. *Introduction to Electrodynamics*. Prentice-Hall, Inc., Englewood Cliffs, NJ, USA, 2 edition, 1989.
- [30] R. L. Kaufmann, W. R. Paterson, and L. A. Frank. Magnetization of the plasma sheet. *Journal of Geophysical Research (Space Physics)*, 109(A18):9212–+, 2004.
- [31] Richard Feynman, Robert B. Leighton, and Matthew L. Sands. *The Feynman Lectures on Physics*. Addison-Wesley, 1963. 3 volumes.
- [32] F. Halzen and A. D. Martin. *Quarks and Leptons*. Wiley, 1985.
- [33] L. H. Ryder. *Quantum Field Theory*. Cambridge University Press, 1985.
- [34] B. V. Somov. *Plasma Astrophysics: Fundamentals and Practice*. Springer, 2006.
- [35] A. Ferriz-Mas and M. Nunez. *Advances in Nonlinear Dynamos*. CRC Press, 2003.
- [36] Shoichi Yoshikawa. Toroidal plasma equilibrium with gravity. *Physics of Fluids*, 24(3):513–516, 1981.
- [37] James C. Maxwell. A dynamical theory of the electromagnetic field. *Royal Society Transactions*, 155, 1864.
- [38] J. R. Melcher. *Continuum Electromechanics*. MIT Press, Cambridge, Mass., 1981.
- [39] R. E. Rosensweig. Magnetic fluids. *Sci. Am.*, 247(4):136–145, 1982.
- [40] H. Grad and H. Rubin. Hydromagnetic equilibria and force-free fields. *Proceedings of the 2nd UN Conf. on the Peaceful Uses of Atomic Energy*, 31:190, 1958.
- [41] V. D. Shafranov. Plasma equilibrium in a magnetic field. *Reviews of Plasma Physics*, 3:103, 1966.